

# The stability and fate of synthesized zero-valent iron nanoparticles in freshwater microcosm system

Deepak Kumar<sup>1</sup> · Abhinav Parashar<sup>1</sup> · Natarajan Chandrasekaran<sup>1</sup> · Amitava Mukherjee<sup>1</sup>

Received: 14 March 2017 / Accepted: 30 June 2017  
© Springer-Verlag GmbH Germany 2017

**Abstract** Zero-valent iron nanoparticles are used for the degradation of organic compounds and the immobilization of metals and metalloids. The lack of information on the effect of nZVI in freshwater system necessitated the risk assessment of zero-valent iron nanoparticles in lake water environment. The present study deals with the stability and fate of synthesized zero-valent iron nanoparticles in the upper and lower layers of freshwater microcosm system at a concentration of 1000 mg L<sup>-1</sup>. The study was divided into two different exposure periods: short-term exposure, up to 24 h after the introduction of nanoparticles, and long-term exposure period up to 180 days (4416 h). Aggregation kinetics of nZVI in freshwater microcosm was studied by measuring the mean hydrodynamic size of the nanoparticles with respect to time. A gradual increase in the particle size with time was observed up to 14 h. The algal population and total chlorophyll content declined for the short exposure period, i.e., 2–24 h, while in the case of longer exposure period, i.e., 24 h to 180 days (4416 h), a gradual increase of both the algal population and total chlorophyll was noted. Five different physico-chemical parameters such as pH, temperature, conductivity, salinity, and total dissolved solids were recorded for 180 days (6 calendar months). The study suggested that the nanoscale zero-valent iron did not exhibit significant toxicity at an exposure concentration of 1000 mg L<sup>-1</sup> on the resident algal

population in the microcosm system over the longer exposure period tested.

**Keywords** Algae · Ecotoxicity · Microcosm · Stability · Zero-valent iron nanoparticles

## Introduction

Nanoscale zero-valent iron (nZVI) has been used increasingly over the last decade to clean polluted water, soil, and sediments (Li et al. 2006; Stefaniuk et al. 2016). nZVI particles offer several advantages for in situ applications because of their large specific surface area, which results in high reaction rates (Xiu et al. 2010). The toxic chemicals can be treated by nZVI particles through adsorption, reduction or a combination of both the processes (Grieger et al. 2010). Organic and inorganic contaminants such as perchlorate, nitrate, polychlorinated hydrocarbons, chromate, chloride, and organic dyes can be easily reduced by nZVI to less harmful compounds (Lacinova et al. 2012; Li et al. 2006).

The distinct catalytic properties of nZVI can have a potentially harmful impact on indigenous organisms when released into the environment (Dinesh et al. 2012; Patil et al. 2016). The recent studies on nZVI illustrated that nZVI was toxic to microorganisms at concentrations as low as few mg L<sup>-1</sup> in pure cultures (Barnes et al. 2010). The interaction of the particles with biointerfaces may decrease both cell mobility and nutrient flow between the cell's exterior and interior compartments (Zanaroli et al. 2012). Additionally, the possible adsorption of nZVI onto the outer cell membranes may lead to increased membrane permeability or even cause disruption of the membrane lipid bilayer (Lee et al. 2008). The major part of the

**Electronic supplementary material** The online version of this article (doi:10.1007/s13205-017-0869-4) contains supplementary material, which is available to authorized users.

✉ Amitava Mukherjee  
amit.mookerjea@gmail.com; amitav@vit.ac.in

<sup>1</sup> Centre for Nanobiotechnology, VIT University,  
Vellore 632014, India

manufactured nZVI enters the environment through their direct injection into the polluted aquifer and soil (Kirschling et al. 2010). It was noted in previous reports that under rare circumstances when the bioavailability of iron was in surplus, oxidative stress can be stimulated, which could influence the algal growth (Jaramillo et al. 2015; Ševců et al. 2011). Earlier studies report on the effect of surplus redox-active iron on the oxidative stress in *Chlorella vulgaris* (Estevez et al. 2001).

Algae represent the first level of the trophic food chain in the aquatic ecological system, and it is one of the most delicate organisms to interact with pollutants. Thus, any harmful effect to this organism may disturb the whole food chain of the ecosystem. Hence, the present study focused on evaluating the aggregation behavior of nZVI in two compartments (upper layer, i.e., 10–15 L and bottom layer, i.e., 0–5 L) in a microcosm system, and its toxic effect towards the resident algal community. The five different physico-chemical parameters (pH, temperature, total dissolved solid, conductivity, and salinity) were analyzed over 24 h (short term, 1 day) followed by 4416-h (long term, 180 days) exposure period to investigate their influence on the behavior and fate of nZVI in natural freshwater. Previous studies on the nano-remediation of Cr(VI) by nZVI employed 1000 mg L<sup>-1</sup> concentration for its efficient functioning (Ravikumar et al. 2016a; Li et al. 2016; Liu et al. 2010, 2012; Shi et al. 2011; Xiu et al. 2010). Hence, the working concentration of synthesized nZVI for the initial exposure was selected as 1000 mg L<sup>-1</sup>.

## Materials and methods

### Materials

Sodium borohydride (NaBH<sub>4</sub>), ferrous sulfate (FeSO<sub>4</sub>·7H<sub>2</sub>O), and EDTA (C<sub>10</sub>H<sub>14</sub>N<sub>2</sub>Na<sub>2</sub>O<sub>8</sub>·2H<sub>2</sub>O) were obtained from Sisco Research Laboratories Pvt. Ltd., India, and the solutions were prepared with deionized water.

### Synthesis of nZVI particles

The nZVI particles were synthesized from FeSO<sub>4</sub> as a starting material. The starting material, Fe<sub>2</sub>SO<sub>4</sub> (150 mL, 0.1 M), and the stabilizing agent, 0.1 M EDTA (100 mL), were prepared and mixed together at a constant temperature of 55 ± 3 °C. Then, the solution was allowed to attain a constant temperature, 50 °C, which has been followed throughout the process. Further, 100 mL of 0.75 M NaBH<sub>4</sub> was added to the reaction mixture. A constant stirring speed of 500 rpm was maintained throughout the reaction. Gradually, the solution turned to light black color by the precipitation of zero-valent iron (Allabaksh et al. 2010). After the

precipitation of ZVI, the solution was allowed to settle down at the room temperature, 26 °C. Further, the supernatant was removed after the centrifugation at 1000 rpm for about 30 min. The solids, which were settled, were washed with absolute ethanol and dried at 100 °C (Ravikumar et al. 2016b).

### Site details

Microcosm study was carried out using the freshwater collected from VIT Lake, Vellore, India. Vellore is located between 12°–15° and 13°–15° northern latitude and between 78°–20° and 79°–50° eastern longitude. It has an average elevation of 216 m. The area has a typical mediterranean climate with mild winter and dry summer. The temperature ranges from as low as 15 °C in the winter months of December–February up to even 43 °C in the summer months of June–November. It has a rainy weather mostly and is humid during the two monsoons: June–August and October–December. The average annual rainfall is around 442 mm.

### Establishment of microcosm

Microcosm experiment was carried out for six calendar months (180 days) from the period of June 2015 to November 2015. In the present study, glass tanks with 15-L capacity were used for the microcosm setup, in which the natural lake water circumstances were simulated (Barnes et al. 2010; Bour et al. 2015). The dimension of the glass tank used for the experiment was 45 × 45 × 45 cm. The tanks were separated into two layers, viz., the upper layer comprises lake water and the lower layer comprises the sediments of the lake. The lake water and sediments used in the present study were collected from the VIT Lake and used for the experiment without any further processing to maintain the biota of the source. Thus, the lower layer of the tank (0–5 L) constitutes the lake sediment without any deportation of the existing biotic and abiotic component, and the upper layer of the tank (10–15 L) comprised of lake water with all the microbial species (bacteria, algae, etc.) as well as suspended organic and inorganic matter. Since the lower layer consisted of sediments and the upper layer had water, it was naturally demarcated on a physical basis. No artificial physical separation was implemented between the two layers. Initially, the prepared tanks were kept in the field for 4 weeks in the open natural condition for acclimatization and used for the experiments. Further, the glass tanks were kept in the field throughout the study. The aim was to make an isolated investigational setup, which can be monitored with no difficulty without polluting the natural environment (Fig. 1).

An exposure concentration of 1000 mg L<sup>-1</sup> nZVI was tested in the study. The stock dispersion of 10000 mg L<sup>-1</sup>

**Fig. 1** Photograph showing microcosm setup under natural conditions



nZVI was prepared in deionized water and was subsequently sonicated using a bath sonicator (CREST Ultra Sonics, USA). From the stock, 1500 mL was added to the experimental microcosm tank to achieve a working dispersion of  $1000 \text{ mg L}^{-1}$  in the experimental setup. To evaluate the changes obtained in the microcosm upon nZVI addition, 20 mL of the samples was collected from the upper layer (10–15 L) and lower layer (0–5 L) as marked on glass tank of the microcosm setup (Fig. 1) and several parameters such as physico-chemical parameters, size of nZVI, and algal population have been analyzed at different time intervals. The removed water sample collected for the analysis was replenished with the source lake water, which was collected and stored separately, to maintain the constant water level of glass tank, i.e., 15-L mark as shown in Fig. 1

In addition, the hydrodynamic size distribution of the particles or particle agglomerates was determined for the working dispersion ( $1000 \text{ mg L}^{-1}$ ) by dynamic light scattering using 90 Plus Particle Size Analyzer (Brookhaven Instruments Corp, USA).

### Physico-chemical parameters

As mentioned, the microcosm setup was kept in natural condition and the five different physico-chemical parameters (pH, TDS, salinity, conductivity, and temperature) were studied throughout the experiment for both, upper and lower, layers of the tanks using the multi-parameter PCSTestr TM

35 (Eutech instrument, Singapore), which has been outlined in Tables S1 and S2, respectively (Supporting information). Initially, all the five parameters were quantified every 2 h till 14 h, after that, it was quantified every 24 h up to 7 days followed by every 7 days up to 180 days (4416 h). The average rainfall during the experiment was recorded and detailed in Table S3 in supporting information.

### Aggregation of particles in lake water

$1000 \text{ mg L}^{-1}$  of nZVI dispersion was added to the glass tank from the stock dispersion of  $10,000 \text{ mg L}^{-1}$ . At every 2-h time interval, 20 mL of water samples was collected from upper and lower layers of the tank till 14 h. The collected water samples were filtered consecutively through a sequence of coarse- to fine-pore-sized filters (20-mm mesh-Whatman no. 1 filter paper–Whatman no. 42 filter paper) and were subjected to particle size analysis using dynamic light scattering.

### Estimation of total iron content

To estimate the total iron content, the water samples were collected from upper and lower layers of the tank at every 2 h time interval up to 14 h. The collected samples were acid digested by heating with  $\text{HNO}_3$  (70%) at  $90^\circ \text{C}$ . The digested samples were then analyzed using atomic absorption spectrophotometry (AAS; PerkinElmer, Analyst 400, USA).

### Estimation of algal cell count

To estimate the effect of nZVI on the algal population of microcosm, 10 mL of the water samples was collected from both, upper and lower, layers of the microcosm system at various time intervals such as every 2 h till 14 h and every 24 h up to 7 days, followed by every 7 days up to 180 days. After following a standard protocol for filtration, the sample was further loaded on to a Neubauer chamber, after placing a cover slip. Then, the total number of intact cells was calculated under a bright-field microscope at  $400\times$  magnification. The percentage viability of the test tanks was computed after its normalization with the viability of the control tanks.

### Estimation of total chlorophyll

Total chlorophyll estimation shows the livability of algal flora in an experimental system. In a particular system, the total chlorophyll estimation is a very straight and sensitive indicator of modifications in the algal population. To evaluate the total chlorophyll, 100 mL of water samples containing the resident algae was collected at specified time intervals. Initially, the water samples were collected every 2 h till 14 h, after that, it was quantified every 24 h up to 7 days, followed by every 7 days up to 180 days (4416 h) from upper as well as lower layers of the glass tanks. The removed water sample was replaced with the lake water to maintain the level of glass tank at 15 L mark as shown in Fig. 1. Total chlorophyll was quantified as per modified OECD guidelines (Organization for Economic Cooperation and Development, 2011) and Fargašová et al. (1999). Chlorophyll was extracted with the solvent, dimethyl formamide (DMF). The extract obtained was further measured at two different wavelengths, such as 649 and 665 nm using a double-beam UV–Vis spectrophotometer (Systronics, India Ltd.) (Fargašová 2001).

### Characterization methods

#### *X-ray powder diffraction*

The X-ray powder diffraction (XRD) analysis was performed using a Bruker Advanced D8 (Germany) diffractometer using  $\text{CuK}\alpha$  radiation ( $\lambda = 1.5418 \text{ \AA}$ ) to identify the structure and composition of the chemically synthesized nZVI. Each sample was scanned within the range of  $20^\circ$ – $80^\circ$ .

#### *Dynamic light scattering analysis*

The size distribution of the synthesized nZVI was measured using dynamic light scattering (DLS) (Horiba, SZ-100, Japan) in the dispersion medium (deionized water).

#### *Scanning electron microscopy*

The surface morphology of synthesized nZVI was observed by a field-emission scanning electron microscope (FESEM; SUPRA 55, Carl Zeiss, Germany). The samples were mounted on metal stubs using a carbon tape and sputter coated with gold in an argon atmosphere for 1 h before analysis.

#### *Energy-dispersive X-ray spectroscopy*

The surface elemental analysis of synthesized nZVI was done by energy-dispersive X-ray spectroscopy (EDX) (Model 51-ADD0011, Oxford Instruments, Germany). The gold sputtering was done before analyzing the samples.

#### *Transmission electron microscopy*

The particle morphology of nZVI was studied with the help of transmission electron microscopy (Philips CM12, Netherlands). The sample was placed onto a delicate carbon-coated copper grid and used for transmission electron microscopic analysis.

### Statistical analysis

All the experiments were performed in triplicates, and all the data points are expressed in terms of mean with standard error (SE). One-way ANOVA followed by Dunnett's and Newman–Keuls post hoc test (as applicable) were further carried out using Prism 6.0 software for each set of experiments to show the significant variations (at  $p < 0.05$ ) at various time points.

## Results

### Characterization of synthesized nZVI nanoparticles

The synthesis of nZVI was confirmed by XRD and SEM–EDX analyses. The XRD analysis demonstrated the crystalline nature of nanoparticles. The  $2\theta$  peak at  $46.48^\circ$  corresponds to the (111) phase of the body-centered cubic structure (BCC) of iron. The acquired XRD pattern was matched with the JCPDS card no. 00-006-0696, confirming that the synthesized nanoparticles were indeed nZVI (Fig. 2). Additionally, the SEM analysis was performed to study the surface morphology of the nZVI. Figure 3 shows that nZVI was of irregular shape with undefined structure and existed as an aggregate. EDX analysis showed that the iron content in the synthesized nZVI was 75.99%. The transmission electron microscopic image of nZVI confirmed (Fig. 4) that they were mostly spherical in shape

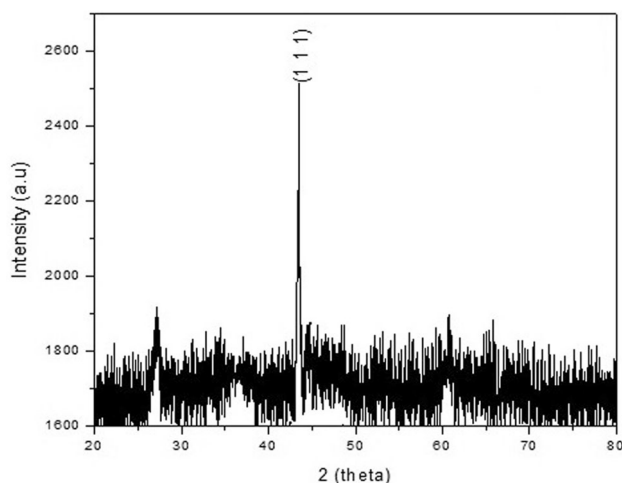


**Fig. 2** XRD image of synthesized zero-valent iron nanoparticles

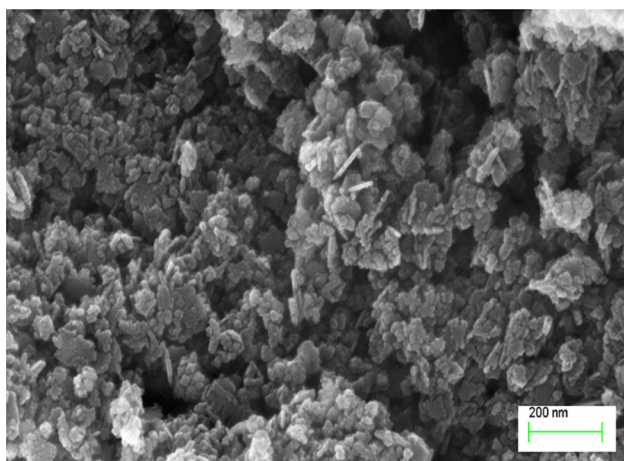


**Fig. 3** Scanning electron micrograph of synthesized zero-valent iron nanoparticles

with size ranging between 32 and 35 nm. The mean hydrodynamic size of the nanoparticles was found to be 254 nm in deionized water as mentioned in our previous report (Ravikumar et al. 2016b).

#### Aggregation kinetics of nZVI in freshwater microcosm system

There was a gradual increase in the particle size with time up to 14 h. The mean hydrodynamic size of the nanoparticles was found to be  $440 \pm 23$ ,  $818 \pm 132$ , and  $966 \pm 99$  nm at 2, 4, and 6 h, respectively, in the upper layer of the system. Thereafter, an increase in the size was observed and the hydrodynamic size reached  $1132 \pm 193$  nm at 8 h,  $1285 \pm 265$  nm at 10 h, and  $2407 \pm 483$  nm at 12 h. Finally, a remarkable increase in the size of the nanoparticles was observed and the size reached up to  $3430 \pm 194$  nm at 14 h (Fig. 5).

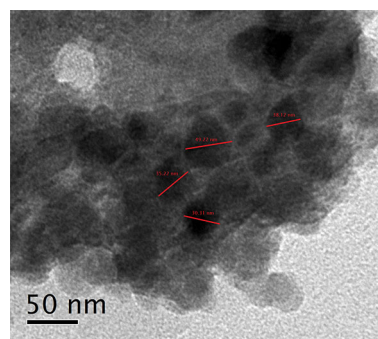


**Fig. 4** Transmission electron micrograph of synthesized zero-valent iron nanoparticles

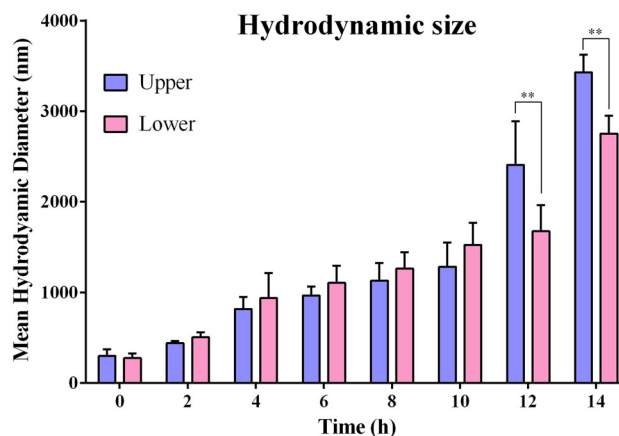


**Fig. 5** Detailed particle size analysis in lake water matrix

Further, the mean hydrodynamic size of nanoparticles in the lower layer was measured to be  $504 \pm 57$ ,  $937 \pm 279$ , and  $1107 \pm 187$  nm at 2, 4, and 6 h, respectively. An increase in the mean hydrodynamic size was observed after 6th hour, and the measured sizes were  $1263 \pm 180$ ,  $1526 \pm 240$ ,  $1674 \pm 287$ , and  $2752 \pm 199$  nm at 8, 10, 12, and 14 h, respectively (Fig. 5).

There was no significant ( $p > 0.05$ ) difference in the particle size between the upper layer and the bottom layers of the microcosm till 10th hour. After 10 h, i.e., at 12th and 14th hour, there was a significant ( $p < 0.01$ ) difference in the particle size observed in both the layers (upper and lower) of the microcosm setup.

#### Total iron content in the upper and layer lowers of the microcosm

Total iron present in the system before addition of the nanoparticles was found to be  $0.1 \text{ mg L}^{-1}$ , whereas after addition of nZVI to the system, soluble iron was measured to be  $620 \pm 0.053$ ,  $380 \pm 0.043$ ,  $80 \pm 0.013$ ,  $30 \pm 0.004$ ,  $10 \pm 0.001$ , and  $10 \pm 0.002 \text{ mg L}^{-1}$  at 0, 2, 4, 6, 8, and 10 h, respectively, in the upper layer of the system (Fig. 6).

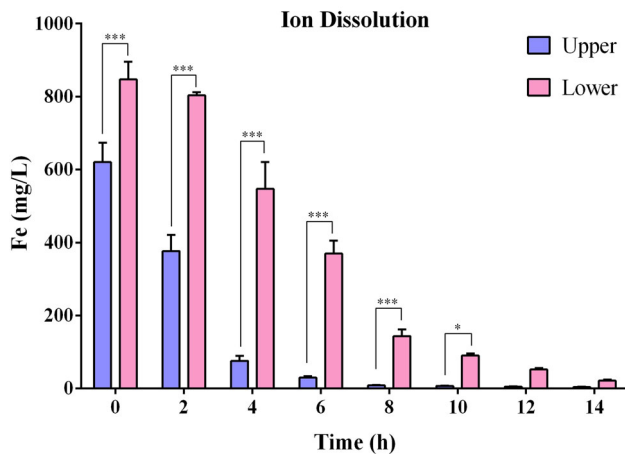


**Fig. 6** Iron dissolution profile of soluble zero-valent iron nanoparticles in lake water matrix

In the lower layer, the total iron content was found to be  $850 \pm 0.048$ ,  $800 \pm 0.009$ ,  $550 \pm 0.073$ ,  $370 \pm 0.035$ ,  $140 \pm 0.019$ ,  $90 \pm 0.006$ ,  $50 \pm 0.004$ , and  $20 \pm 0.003 \text{ mg L}^{-1}$  at 0, 2, 4, 6, 8, 10, 12, and 14 h, respectively (Fig. 6).

The result compared between the upper and lower layers of the microcosm setup for ion dissolution showed a significant ( $p < 0.001$ ) difference in the Fe concentration up to 8th hour. Further, at 10th hour, the difference in Fe concentration was significantly ( $p < 0.05$ ) higher in the lower layer. There was no significant difference in Fe concentration at 12th and 14th hour in both the layers of experimental setup.

### Effect of nZVI on algal population and chlorophyll estimation

The toxic effect of nZVI on the resident algal population was analyzed by calculating the number of viable cells and also by quantifying the total chlorophyll present in both, the upper and lower, layers of the freshwater microcosm system. The algal population and total chlorophyll were quantified after the addition of nanoparticles. Interestingly, the algal population (Fig. 7) and total chlorophyll (Fig. 8) were noted to be decreasing with respect to time for the short exposure period, i.e., 2–24 h. In the case of the longer period, i.e., 24 h to 180 days (4416 h), a gradual increase of the algal population from both, upper (Fig. 7a) and lower (Fig. 7b), layers and total chlorophyll in both layers, i.e., upper (Fig. 8a) and lower (Fig. 8b), of the system was observed. When the algal population was compared between the upper (Fig. 7a) and lower layers (Fig. 7b) of the system, it was found that the toxicity was lesser in the lower layers till 24 h, and the toxicity was found to be decreasing in both the layers with an increase in time up to 180 days. The result, therefore, supports that the

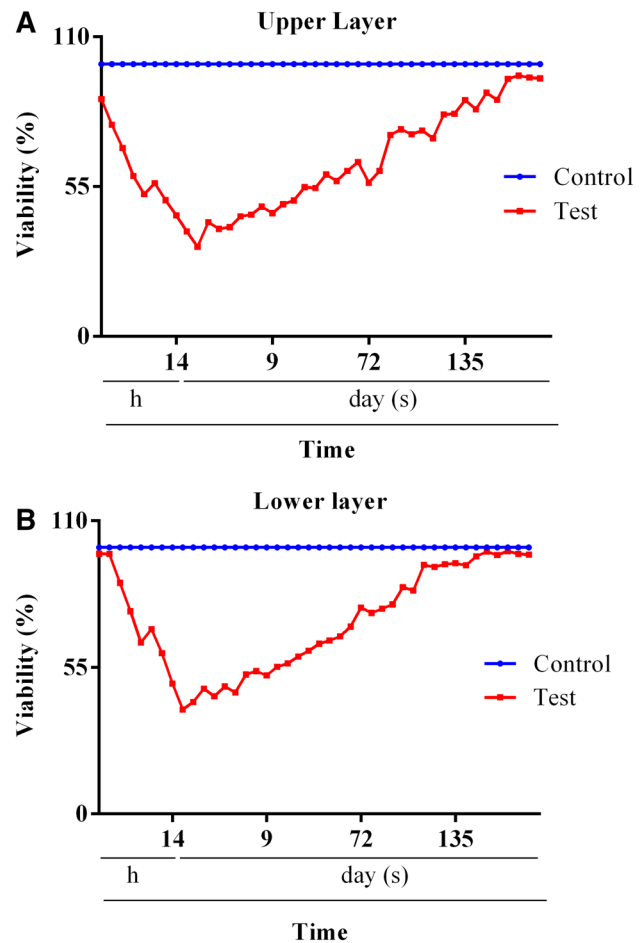


**Fig. 7** Depiction of dose-associated impact of zero-valent iron nanoparticles on freshwater algae **a** upper layer, **b** lower layer

differential toxicity of nZVI in both the layers may be due to the variation in the bioavailability of the iron (Kumar et al. 2014; Marsalek et al. 2012). The studies also confirmed that the nZVI was highly unstable and behaved as a bulk particle with increase in time.

### Discussion

#### Preliminary observations on the effect of aggregation on freshwater-resident algal population

The nZVI concentration ( $1000 \text{ mg L}^{-1}$ ) was selected according to the previous experiment to remove Cr(VI) from contaminated water samples (Ravikumar et al. 2016a, b). The effect of aggregation–settling of the particles in the microcosm was monitored with time for this fixed concentration of particles. Since the microcosm was open to the environment, the effects of weathering conditions also played a definite role in deciding the physico-

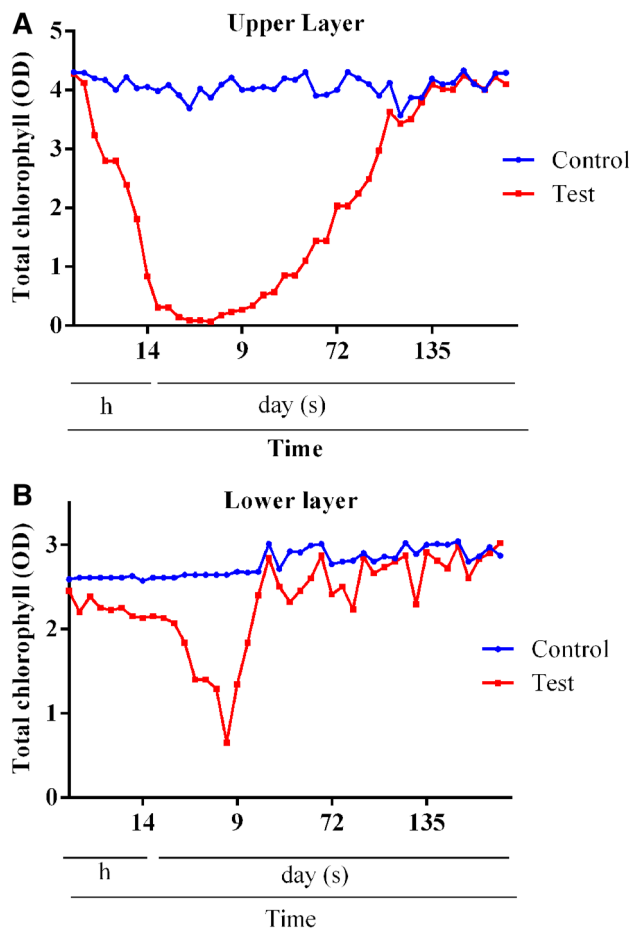


**Fig. 8** Depiction of dose-associated impact of zero-valent iron nanoparticles on total chlorophyll **a** upper layer, **b** lower layer

chemical behavior of the particles in the aquatic system. According to the previous reports, large-sized particles behave as bulk particles and also the toxic effect will decrease with increase in the size of nanoparticles (Brunner et al. 2006; Karakoti et al. 2006). Therefore, the particle size analysis was stopped beyond 14 h since the size range exceeded beyond 2000 nm. It has been reported that uncoated or bare nZVI are prone to quick aggregation and agglomeration, frequently forming micro-sized fractal aggregates (Phenrat et al. 2007; Sun et al. 2006), which may subsequently lead to a significant loss in reactivity and decreased environmental mobility (Theron et al. 2008; Grieger et al. 2010). It is also to be noted that pH plays a significant role in the ion dissolution of the nanoparticles (Kumar et al. 2014; Pakrashi et al. 2012). It was also observed that the total Fe concentration in the microcosm system was nearly negligible in the upper layer after the 10th hour. On the other hand, in the lower layer, the presence of iron content was 50 and 20 mg L<sup>-1</sup> at 12 and 14 h, respectively, which showed that the iron nanoparticles were aggregating and getting settled in the lower layer of the system.

### Ecological implications of particle aggregation and bioavailability

As discussed in previous reviews on environmental implications of zero-valent iron nanoparticles (Grieger et al. 2010; Stefaniuk et al. 2016), there is limited number of ecotoxicity studies on freshwater organisms to critically understand the hazardous potential of the particles. To date, there are no studies on the long-term effects of nZVI particles in freshwater microcosm systems. The current study assumes importance in this context.

The colloidal stability and agglomeration/aggregation in the aquatic system would strongly influence the biological reactivity and toxicity potential of the nZVI particles. The quantity of total iron present in the system was a direct indicator of bioavailability of the nZVI particles in the different layers of the system. The negative impact of the particles would depend on their bioavailability in the test system. The bioavailability and form of the nanoparticles play an important role in their toxicity (Üzüüm et al. 2008). In this study, it was noted that the synthesized nZVI experienced an extensive increase in the particle size after 2nd hour in the microcosm system. The toxic effect of 1000 mg L<sup>-1</sup> of nZVI on algae was observed to be increasing up to 24 h in both, upper and lower, layers of the microcosm system as indicated in Fig. 7. Afterwards, the toxic effects gradually decreased with increase in the exposure time up to 180 days for the upper and lower layers. Though higher concentration of Fe, i.e., nanoparticles was available in the lower layer due to aggregation and consequent settling, the toxicity on resident algal population was slightly lower in the lower layer. The revival of the cell viability and total chlorophyll content began earlier than in the upper layer. This may be due to decreased toxic effects of the particle aggregates in the lower layer. In the current study, the purported decline in toxicity with time in the long-term assessment proves that the possible agglomeration/settling of the particles perhaps steadily decreased their bioavailability.

In spite of the increase in the use of nZVI materials and their capacity to influence the toxic effects in both water and soil organisms (Kirschling et al. 2010), there have been scattered reports regarding the negative effects of nZVI on bacteria (Davenport et al. 2000) and algae (Marsalek et al. 2012). In case of algal toxicity assessment, the effect of synthesized iron nanoparticles on the total chlorophyll content has not been mentioned in the literature so far. Nanoparticles might have indirect and direct effects on the resident algal population in the system. The bioavailability of the nanoparticles may induce oxidative stress, which affects the algal growth and cause adverse impacts on the natural phytoplankton. Previous studies have demonstrated that nZVI forms a coating around the algae, leading to the

shutdown of photo system II, thereby inhibiting photosynthesis, which eventually effects the cell growth. The variation in the different parameters has been represented in Tables S1 and S2 for upper and lower layers, respectively. However, since the microcosm study was conducted under uncontrolled field conditions, it would be difficult to arrive at a generalized conclusion regarding the effects of pH, salinity, temperature on the algal growth in the presence of the nanoparticles.

Distinctive differences were observed in the aggregation behavior in short exposure duration, mainly based on the crystalline phases of the nanoparticles, which influenced their toxicological impact on the microalgae in the system. This was a preliminary study performed at natural conditions to evaluate the aggregation and toxicity of nZVI (1000 mg L<sup>-1</sup>) on algal population after 180 days. The study indicated a rapid aggregation of ZVI nanoparticles, and a reduction of algal population at short term, whereas after 24 h, the algal population showed a gradual revival. Comparing between the upper and lower layer of the microcosm, the later showed less toxicity. Due to the lack of manual control and complex nature of ecological parameters in a microcosm setup, it is quite complicated to obtain a definite conclusion from these types of studies.

**Acknowledgements** We acknowledge Department of Science and Technology-Science and Engineering Research Board (DST-SERB) [SB/S3/ME/0019/13], Government of India for providing the grant throughout this research work. We also acknowledge VIT University, Vellore for providing facilities to carry out our work.

#### Compliance with ethical standards

**Conflict of interest** The authors declare that they have no conflict of interests.

#### References

- Allabaksh M, Mandal B, Kesarla M, Kumar K, Reddy P (2010) Preparation of stable zero valent iron nanoparticles using different chelating agents. *J Chem Pharm Res* 2:67–74
- Barnes RJ, van der Gast CJ, Riba O, Lehtovirta LE, Prosser JJ, Dobson PJ, Thompson IP (2010) The impact of zero-valent iron nanoparticles on a river water bacterial community. *J Hazard Mater* 184:73–80
- Bour A, Mouchet F, Silvestre J, Gauthier L, Pinelli E (2015) Environmentally relevant approaches to assess nanoparticles ecotoxicity: a review. *J Hazard Mater* 283:764–777
- Brunner TJ et al (2006) In vitro cytotoxicity of oxide nanoparticles: comparison to asbestos, silica, and the effect of particle solubility. *Environ Sci Technol* 40:4374–4381
- Davenport AJ, Oblonsky LJ, Ryan MP, Toney MF (2000) The structure of the passive film that forms on iron in aqueous environments. *J Electrochem Soc* 147:2162–2173
- Dinesh R, Anandaraj M, Srinivasan V, Hamza S (2012) Engineered nanoparticles in the soil and their potential implications to microbial activity. *Geoderma* 173:19–27
- Estevez MS, Malanga G, Puntarulo S (2001) Iron-dependent oxidative stress in *Chlorella vulgaris*. *Plant Sci* 161:9–17
- Fargašová A (2001) Phytotoxic effects of Cd, Zn, Pb, Cu and Fe on *Sinapis alba* L. seedlings and their accumulation in roots and shoots. *Biol Plant* 44:471–473
- Fargašová A, Bumbálová A, Havránek E (1999) Ecotoxicological effects and uptake of metals (Cu<sup>+</sup>, Cu<sup>2+</sup>, Mn<sup>2+</sup>, Mo<sup>6+</sup>, Ni<sup>2+</sup>, V<sup>5+</sup>) in freshwater alga *Scenedesmus quadricauda*. *Chemosphere* 38:1165–1173
- Grieger KD, Fjordbøge A, Hartmann NB, Eriksson E, Bjerg PL, Baun A (2010) Environmental benefits and risks of zero-valent iron nanoparticles (nZVI) for in situ remediation: risk mitigation or trade-off? *J Contam Hydrol* 118:165–183
- Jaramillo Á, Briones L, Andrews M, Arredondo M, Olivares M, Brito A, Pizarro F (2015) Effect of phytic acid, tannic acid and pectin on fasting iron bioavailability both in the presence and absence of calcium. *J Trace Elem Med Biol* 30:112–117
- Karakoti A, Hench L, Seal S (2006) The potential toxicity of nanomaterials—the role of surfaces. *JOM* 58:77–82
- Kirschling TL, Gregory KB, Minkley J, Edwin G, Lowry GV, Tilton RD (2010) Impact of nanoscale zero valent iron on geochemistry and microbial populations in trichloroethylene contaminated aquifer materials. *Environ Sci Technol* 44:3474–3480
- Kumar D et al (2014) A temporal study on the effects of TiO<sub>2</sub> nanoparticles in a fresh water microcosm. *Proc Natl Acad Sci India Sect B* 2:1–6
- Lacinova L, Kvapil P, Cernik M (2012) A field comparison of two reductive dechlorination (zero-valent iron and lactate) methods. *Environ Technol* 33:741–749
- Lee C, Kim JY, Lee WI, Nelson KL, Yoon J, Sedlak DL (2008) Bactericidal effect of zero-valent iron nanoparticles on *Escherichia coli*. *Environ Sci Technol* 42:4927–4933
- Li X-g, Elliott DW, Zhang W-x (2006) Zero-valent iron nanoparticles for abatement of environmental pollutants: materials and engineering aspects. *Crit Rev Solid State Mater Sci* 31:111–122
- Li X, Ai L, Jiang J (2016) Nanoscale zerovalent iron decorated on graphene nanosheets for Cr(VI) removal from aqueous solution: surface corrosion retard induced the enhanced performance. *Chem Eng J* 288:789–797
- Liu T, Zhao L, Sun D, Tan X (2010) Entrapment of nanoscale zero-valent iron in chitosan beads for hexavalent chromium removal from wastewater. *J Hazard Mater* 184:724–730
- Liu T, Wang Z-L, Zhao L, Yang X (2012) Enhanced chitosan/Fe<sup>0</sup>-nanoparticles beads for hexavalent chromium removal from wastewater. *Chem Eng J* 189:196–202
- Marsalek B, Jancula D, Marsalkova E, Mashlan M, Safarova K, Tucek J, Zboril R (2012) Multimodal action and selective toxicity of zerovalent iron nanoparticles against cyanobacteria. *Environ Sci Technol* 46:2316–2323
- Pakrashi S, Dalai S, Sneha B, Chandrasekaran N, Mukherjee A (2012) A temporal study on fate of Al<sub>2</sub>O<sub>3</sub> nanoparticles in a fresh water microcosm at environmentally relevant low concentrations. *Ecotoxicol Environ Saf* 84:70–77
- Patil SS, Shedbalkar UU, Truskewycz A, Chopade BA, Ball AS (2016) Nanoparticles for environmental clean-up: a review of potential risks and emerging solutions. *Environ Technol Inn* 5:10–21
- Phenrat T, Saleh N, Sirk K, Tilton RD, Lowry GV (2007) Aggregation and sedimentation of aqueous nanoscale zerovalent iron dispersions. *Environ Sci Technol* 41:284–290
- Ravikumar KVG, Kumar D, Kumar G, Pulimi M, Chandrasekaran N, Mukherjee A (2016a) Enhanced Cr(VI) removal by nano zero valent iron immobilized alginate beads in presence of biofilm in a continuous flow reactor. *Ind Eng Chem Res* 55(20):5973–5982
- Ravikumar K, Kumar D, Rajeshwari A, Madhu G, Mrudula P, Chandrasekaran N, Mukherjee A (2016b) A comparative study

- with biologically and chemically synthesized nZVI: applications in Cr(VI) removal and ecotoxicity assessment using indigenous microorganisms from chromium-contaminated site. *Environ Sci Pollut Res* 23:2613–2627
- Ševců A, El-Temsah YS, Joner EJ, Černík M (2011) Oxidative stress induced in microorganisms by zero-valent iron nanoparticles. *Microbes Environ* 26:271–281
- Shi L-n, Zhang X, Chen Z-l (2011) Removal of chromium (VI) from wastewater using bentonite-supported nanoscale zero-valent iron. *Water Res* 45:886–892
- Stefaniuk M, Oleszczuk P, Ok YS (2016) Review on nano zerovalent iron (nZVI): from synthesis to environmental applications. *Chem Eng J* 287:618–632
- Sun H, Wang L, Zhang R, Sui J, Xu G (2006) Treatment of groundwater polluted by arsenic compounds by zero valent iron. *J Hazard Mater* 129:297–303
- Theron J, Walker J, Cloete T (2008) Nanotechnology and water treatment: applications and emerging opportunities. *Crit Rev Microbiol* 34:43–69
- Üzümlü Ç, Shahwan T, Eroğlu AE, Lieberwirth I, Scott TB, Hallam KR (2008) Application of zero-valent iron nanoparticles for the removal of aqueous Co<sup>2+</sup> ions under various experimental conditions. *Chem Eng J* 144:213–220
- Xiu Z-m, Jin Z-h, Li T-l, Mahendra S, Lowry GV, Alvarez PJ (2010) Effects of nano-scale zero-valent iron particles on a mixed culture dechlorinating trichloroethylene. *Bioresour Technol* 101:1141–1146
- Zanaroli G, Negroni A, Vignola M, Nuzzo A, Shu HY, Fava F (2012) Enhancement of microbial reductive dechlorination of polychlorinated biphenyls (PCBs) in a marine sediment by nanoscale zerovalent iron (NZVI) particles. *J Chem Technol Biotechnol* 87:1246–1253